nature communications

Article

https://doi.org/10.1038/s41467-025-56584-5

A synthetic chronogenetic gene circuit for programmed circadian drug delivery

Received: 7 December 2022

Accepted: 20 January 2025

Published online: 07 February 2025

Check for updates

Lara Pferdehirt[1,2,3,4], Anna R. Damato[5], Kristin L. Lenz[1,2,3], Maria F. Gonzalez-Aponte[5], Daniel Palmer[1,2,3,4], Qing-Jun Meng[6], Erik D. Herzog[5] & Farshid Guilak[1,2,3,4]

Circadian medicine, the delivery of therapeutic interventions based on an individual's daily rhythms, has shown improved efficacy and reduced side-effects for various treatments. Rheumatoid arthritis and other inflammatory diseases are characterized by diurnal changes in cytokines, leading to inflammatory flares, with peak disease activity in the early morning. Using a combination of synthetic biology and tissue engineering, we developed circadian-based gene circuits, termed "chronogenetics", that express a prescribed transgene downstream of the core clock gene promoter, *Period2 (Per2)*. Gene circuits were transduced into induced pluripotent stem cells that were tissue-engineered into cartilage constructs. Our anti-inflammatory chronogenetic constructs produced therapeutic concentrations of interleukin-1 receptor antagonist in vitro. Once implanted in vivo, the constructs expressed circadian rhythms and entrained to daily light cycles, producing daily increases in biologic drug at the peak of *Per2* expression. This approach represents the development of a cell-based chronogenetic therapy for various applications in circadian medicine.

Circadian medicine, or the delivery of therapeutic interventions based on an individual's circadian rhythm, is emerging as an important method for minimizing side effects and increasing efficacy of drugs[1]. Circadian rhythms are generated by an intracellular genetic timing mechanism that operates on a roughly 24-h period and exists within nearly all cells in the body[2–4]. The core clock genes, including transcriptional activators *Bmal1* and *Clock*, and repressors *Per1/2* and *Cry1/2*, create an auto-regulatory negative feedback loop that drives daily transcription of clock-controlled genes such as *Nr1d1 and Nr1d2, Dbp*, and *Nfil3*[3,4]. Many tissue-specific clock-controlled genes are involved in maintaining tissue homeostasis and their disruption is associated with various disease processes[2,5–9].

Approximately 50% of mammalian genes are expressed with 24-h rhythms in at least one tissue and their expression is regulated in some way by the circadian clock[10]. Therefore, there has been an increase in research trying to understand the importance of therapeutic delivery in alignment with circadian rhythms. Recently, it was found that over half (56) of the top 100 selling drugs in the United States target the product of a circadian gene[11], spurring additional research and clinical trials examining the effects of timed delivery of drugs based on circadian rhythms (e.g., circadian medicine or chronotherapy) to increase their efficacy and minimize side effects[5,8,10–15]. Increasing evidence has shown that time of day is critical to outcomes in a number of therapeutic interventions, including statins in lowering cholesterol, hypertension, asthma, pain killers for osteoarthritis[16], heart surgery[17], cardiovascular disease treatment[11], and cancer treatment[18–20].

In musculoskeletal tissues such as articular cartilage, bone, or the intervertebral disc, circadian rhythms are essential for normal

[1]Department of Orthopedic Surgery, Washington University School of Medicine, St. Louis, MO, USA. [2]Shriners Hospitals for Children - Saint Louis, St. Louis, MO, USA. [3]Center of Regenerative Medicine, Washington University School of Medicine, St. Louis, MO, USA. [4]Department of Biomedical Engineering, Washington University, St. Louis, MO, USA. [5]Department of Biology, Washington University, St. Louis, MO, USA. [6]Wellcome Centre for Cell Matrix Research, Division of Cell Matrix Biology and Regenerative Medicine, Faculty of Biology, Medicine and Health, University of Manchester, Manchester, UK.
e-mail: guilak@wustl.edu

physiology, and disruption of the core clock genes, even in these peripheral tissues, causes loss of tissue homeostasis and the onset of diseases[5,21]. Furthermore, in disease conditions, such as rheumatoid arthritis (RA) and osteoarthritis (OA), circadian expression patterns in cytokines results in diurnal patterns in the intensity of symptoms, with inflammatory flares typically occurring in the early morning[5,8,12,13,22]. These findings have motivated the development and testing of circadian medicine for RA. In trials of non-steroidal anti-inflammatory drugs (NSAIDs) or methotrexate, patients that took these drugs at night (i.e., a few hours before the peak of the flare) showed improved outcomes and reduced adverse events in response to the drugs. Additionally, patients who received drugs at night instead of the morning to combat the matinal increase in interleukin 6 reported reduced joint pain[15]. Therefore, there is a need to develop and test systems for timed delivery of biologics for enhanced efficacy in musculoskeletal diseases such as RA. Additionally, this timed delivery needs to be personalized to individuals' daily rhythms for ultimate efficacy. Unfortunately, the process of taking drugs at specific times of day can be difficult to maintain since it requires daily injections or delivery of drugs at inconvenient times. This challenge can lead to lapses in patient compliance and poor adoption of the regimen by physicians. With recent advances in synthetic biology and genetic engineering, cell-based therapies that harness cells for controlled, and long-lasting delivery of prescribed biologic drugs can be a promising approach to ensure drug delivery in response to specific exogenous stimuli such as inflammation [e.g.[23],] or at specific times of day and over specific frequencies.

In this study, we developed a bioartificial implant using stem cells with programmed synthetic gene circuits capable of circadian delivery of biologic drugs as a chronogenetic therapy. Based on the cell's own circadian cycles, the system uses a lentiviral synthetic gene circuit driven by the core clock gene, *Per2*, to produce interleukin-1 receptor antagonist (IL-1Ra) as an anti-inflammatory approach to target RA (*Per2*-IL1Ra:Luc) (Fig. 1). This chronogenetic circuit contained a 2 A linker to produce luciferase in addition to the therapeutic drug for circadian monitoring. We first examined the circadian oscillations of the circuit through bioluminescence in transduced murine induced pluripotent stem cells (miPSCs) differentiated into tissue-engineered cartilage. We then characterized the *Per2*-IL1Ra:Luc circuit in vitro to ensure oscillating production of IL-1Ra and to determine if this circuit could maintain its circadian clock in the presence of inflammatory cytokines, which has previously been shown to disrupt the clock[24,25]. Finally, we tested our *Per2*-IL1Ra:Luc circuit in vivo to understand tissue-engineered cartilage circadian clock entrainment to the host and the ability for timed drug delivery and IL-1Ra concentrations in the serum. We showed the ability of this chronogenetic circuit to deliver our therapeutic biologic at specific times of day, driven by *Per2* expression both in vitro and in vivo. This chronogenetic synthetic gene circuit offers a cell-based therapy, driven by the circadian clock, for chronotherapy, providing controlled biologic delivery at prescribed times of day.

Results

Characterization of synthetic chronogenetic reporter circuits and tissue engineered cartilage

To first create chronogenetic circuits, we engineered cartilage cells expressing *Per2*-IL1Ra:Luc and tracked *Per2* gene expression as bioluminescence intensity (BLI) continuously for 60 h. *Per2*-IL1Ra:Luc cells showed circadian oscillations ($n = 13$, 23.4 ± 0.35 h period, Fig. 2B, Supplementary Movie 1) similar to cells expressing a *Per2*-Luc circuit ($n = 3$, 23.25 ± 1 h period, Fig. 2A). BLI of the constitutive control EF1α-Luc constructs showed high bioluminescence, but no daily oscillations ($n = 6$, Supplementary Fig. S1D). These results indicate that the chronogenetic circuit directly follows *Per2* expression within individual cells. We next measured sulfated glycosaminoglycans (sGAG), a main component of the cartilage extracellular matrix, and found that non-transduced (NT), *Per2*-Luc, and *Per2*-IL1Ra:Luc pellets showed similar rich red stain for sGAGs ($n = 4$/group, Fig. 2C) and sGAG content ($n = 7$/group, Fig. 2D). Additionally, we measured collagen type II, a primary component of articular cartilage, and found that NT and *Per2*-IL1Ra:Luc pellets showed similar immunolabeling for collagen type II ($n = 2$-3/group, Fig. 2E). We conclude that our lentiviral chronogenetic therapy did not impair tissue-engineered cartilage formation and that our chronogenetic circuit, *Per2*-IL1Ra:Luc, functions to express luciferase in phase with the clock gene *Per2*.

Synthetic chronogenetic circuit produces IL-1Ra in a circadian manner

We next measured the ability of our *Per2*-IL1Ra:Luc chronogenetic circuit to produce IL-1Ra at different concentrations over time in vitro. Because inflammatory cytokines such as IL-1 can disrupt the circadian clock in native cartilage tissue or tissue-engineered constructs[24,25], we also tested the ability of the *Per2*-IL1Ra:Luc circuit to maintain its oscillations in the presence of IL-1. We found the BLI of the *Per2*-IL1Ra:Luc circuit pre-cytokine was circadian ($n = 10$, pre-cytokine period = 21.9 ± 1.8 h, Fig. 3B) and that the circuit maintained circadian oscillations after the addition of IL-1 ($n = 6$, period = 27.7 ± 7.06 h, Fig. 3B). To quantify the impact of IL-1 on circadian rhythm amplitude, we compared the peak-trough amplitude in the 24 h preceding and 24 h after treatment. This ratio was similar between IL-1 treated cells, untreated cells, and cells treated with PBS (Fig. 3C). Thus, the chronogenetic circuit protected against IL-1 induced loss of daily rhythms.

To determine the production of IL-1Ra, our therapeutic drug, we collected the media from *Per2*-IL1Ra:Luc constructs and collected the constructs for gene expression every 3 h for 72 h. *Per2*-IL1Ra:Luc constructs had increased *Il1rn* gene expression compared to NT controls ($n = 6$/group, $p < 0.001$, Fig. 3D). Additionally, *Il1rn* expression in our chronogenetic circuit showed circadian oscillations and a significant difference between peak and trough of the *Il1rn* expression ($p < 0.05$, Fig. 3D) with a period of 22.8 ± 3.6 h (mean ± SEM). Importantly, IL-1Ra production followed a similar oscillation to *Il1rn* gene expression and maintained a roughly 24-hour period of IL-1Ra expression driven by the circadian clock ($n = 6$, period = 22.5 ± 2.9 h, ARSER algorithm, $p = 0.03$, Fig. 3E). When we measured the rate of IL-1Ra synthesis to account for accumulation of IL-1Ra in the media over time, we found IL-1Ra synthesis peaked around 33 and 63 h ($p < 0.04$), with troughs around 42 and 57 h ($p < 0.01$, Fig. 3E), with a 2-fold change in protein abundance in IL1Ra between peak and trough. These findings confirm the ability of a synthetic gene circuit to produce a therapeutic biologic drug with a daily rhythm in vitro.

Chronogenetic IL-1Ra delivery and entrainment in vivo

Following the in vitro studies, we tested the effectiveness of this chronogenetic therapy approach in vivo for both drug delivery and its ability to synchronize to the circadian clock of the host to deliver the drug at prescribed times of day. We implanted *Per2*-IL1Ra:Luc constructs subcutaneously into the flanks of C57BL/6 J mice (Jackson Laboratories, Bar Harbor, Maine) and imaged bioluminescence three days following implantation from the constructs for 36 h. We found daily rhythms in *Per2*-driven bioluminescence, peaking around dusk with a 2.5-fold increase in BLI compared to trough (ZT13, $n = 7$, Fig. 4C, H). We next assayed for IL-1Ra protein levels in serum through serial blood draws at 4 h post bioluminescence peak and trough (Fig. 4B, D). IL-1Ra concentration in the serum was 3.8 ± 0.7-fold higher around the peak, compared to trough, of *Per2* expression ($n = 7$, $p = 0.0096$, Fig. 4D).

To test if the implanted constructs synchronize to the host's daily rhythm, we reversed the light schedule from 7a lights on/7p lights off (light/dark) to 8a lights off/8p lights on (dark/light). For a week prior to this transition and for a month following, mouse wheel-running

https://doi.org/10.1038/s41467-025-56584-5

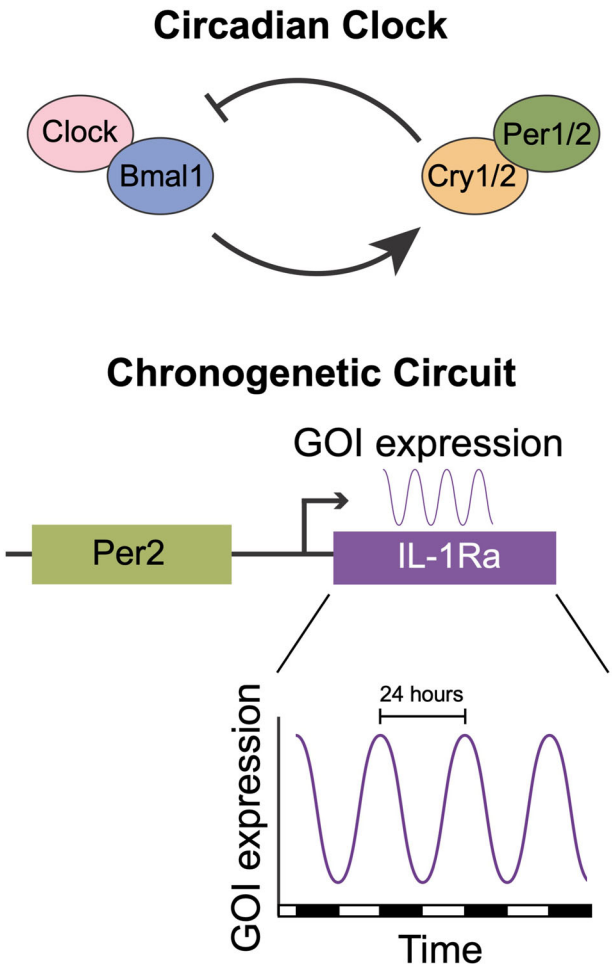

Fig. 1 | Cell-based circadian medicine approach. A therapeutic chronogenetic circuit was created and transduced into murine induced pluripotent stem cells (miPSCs) using lentivirus. These miPSCs were then differentiated into tissue engineered cartilage. The circuit was driven by the *Per2* promoter, activated by core clock component *Per2* and produced both a luciferase reporter and the therapeutic drug, IL-1Ra. The *Per2*-IL1Ra:Luc circuit is capable of delivering an anti-inflammatory drug to target inflammatory flares.

actigraphy was tracked to monitor circadian entrainment to the reversed light/dark cycle. Within one-week post-schedule shift, all mice were once again active during the new dark phase and inactive in the light (Fig. 4B). Following confirmation of re-entrainment via wheel running, the BLI of the implanted constructs was re-assessed. Bioluminescence imaging of constructs showed pellet entrainment to mouse locomotor activity, with BLI peaking at ZT13, as observed previously (Fig. 4C). Serum was again collected for IL-1Ra concentration 4 hours post BLI peak and trough apart and IL-1Ra concentration was significantly increased during peak expression of *Per2* compared to trough ($n = 7$, $p = 0.004$, Fig. 4E). We chose to sample 4-h after the daily peak and trough of bioluminescence to allow time for translation of IL-1Ra. After 21 days of implantation, constructs were removed from the mice and subject to Safranin-O staining or immunohistochemistry for collagen type II. We found that constructs maintained their chondrogenic tissue even after implantation (Fig. 4F, G). Two additional cohorts of mice were implanted with constructs in the flank, one in a reverse LD schedule and the other in a standard LD schedule. Peak timing remained consistent across all three implant cohorts ($n = 12$ mice, Supplementary Fig. S1C). Furthermore, constructs transduced with a constitutive reporter (EF1α-Luc) did not show daily rhythms in bioluminescence in vitro ($n = 4$, Supplementary Fig. S1C) or in vivo ($n = 6$, Supplementary Fig. S1E). These results were consistent over a five-day recording, with subcutaneously implanted *Per2*-IL1Ra:Luc constructs showing circadian oscillations ($n = 5$, period = 23.92 h, Circadian R^2 value 0.71 ± 0.03) and subcutaneously implanted EF1α-Luc constructs showing no circadian rhythm ($n = 5$, Circadian $R^2 = 0.36 \pm 0.07$) (Supplementary Fig. S2). Taken together, these results show the ability of our synthetic circuit to deliver IL-1Ra at different times of day, tracking with the clock component *Per2*, and the ability of our drug delivery system, a tissue engineered pellet, to entrain to the host for prescribed time of day treatment and to persist for at least 28 days in vivo.

Discussion

Building on the principles of circadian medicine, we used synthetic biology to develop cell-based chronogenetic therapies that are capable of delivering biologic drugs at prescribed times, tracking with circadian rhythms. While the notion of taking drugs based on circadian rhythms is gaining popularity, the inconvenient times and need to take the drugs at the same time each day makes it difficult for patients to adhere to the chronotherapy approach. Using a stem cell-based implant, we created a system to deliver drugs autonomously at specific times to provide localized and timed delivery of the drug. Specifically, we determined that the circadian *Per2* promoter can be used to drive daily gene expression and protein production in engineered cells. Driven gene expression peaks about 9 h before protein. These cells, when implanted, integrate to synchronize to the body's daily rhythms and last at least 28 days. In previous studies, we showed persistence and activation of similar constructs, engineered from iPSCs, for 6 months in vivo, indicating the potential for long-lasting, autonomous drug delivery in such a cell-based system[26]. This approach can be used for disease targeting where symptoms or disease severity changes over the day and could be used for more effective delivery of a range of biologic drugs such as growth factors or drugs targeting tissue homeostasis.

Our chronogenetic gene circuit was capable of delivering the anti-inflammatory cytokine IL-1Ra in a timed and oscillating manner through different concentrations of protein in the serum. The decision to implant our tissue-engineered cell therapy subcutaneously was due to the fact that RA is a systemic inflammatory disease, requiring systemic mitigation instead of localized therapy. Additionally, previous work has shown that subcutaneous implantation of tissue-engineered systems that can produce IL-1Ra can effectively mitigate inflammation, pain, and structural damage of RA[26]. This system can be expanded beyond applications in RA and can be used for any inflammatory disease where there are inflammatory flares driven by the circadian clock[11,16,27–29]. Additionally, this type of system can be used to deliver different concentrations of drugs at different times. It is also important to note that other stimuli such as mechanical loading may occur in a diurnal manner[30] and could be implemented as a mechanogenetic system[31] to function in a synergistic manner with chronogenetic gene circuits as presented here.

Importantly, we also evaluated the ability of our tissue engineered cell therapy to entrain to its host, as this is important when producing chronogenetic therapies driven by the host circadian clock. Here we see that our tissue engineered constructs synchronize to the host and can continue to entrain even with shifts in circadian rhythms, consistent with prior results indicating that implanted cells can synchronize to the host[32]. The ability of the tissue engineered system to entrain with the mouse circadian clock, even following reversal of the light/dark cycle, is important in the ability of our tissue engineered systems to maintain prescribed drug delivery that is synchronized to personalized circadian rhythms. This characteristic is critical for consistent delivery timing even during perturbations or shifts in circadian rhythms that can happen with shift work, circadian disorders, different chronotypes, and other disease pathologies that can affect the circadian clock.

https://doi.org/10.1038/s41467-025-56584-5

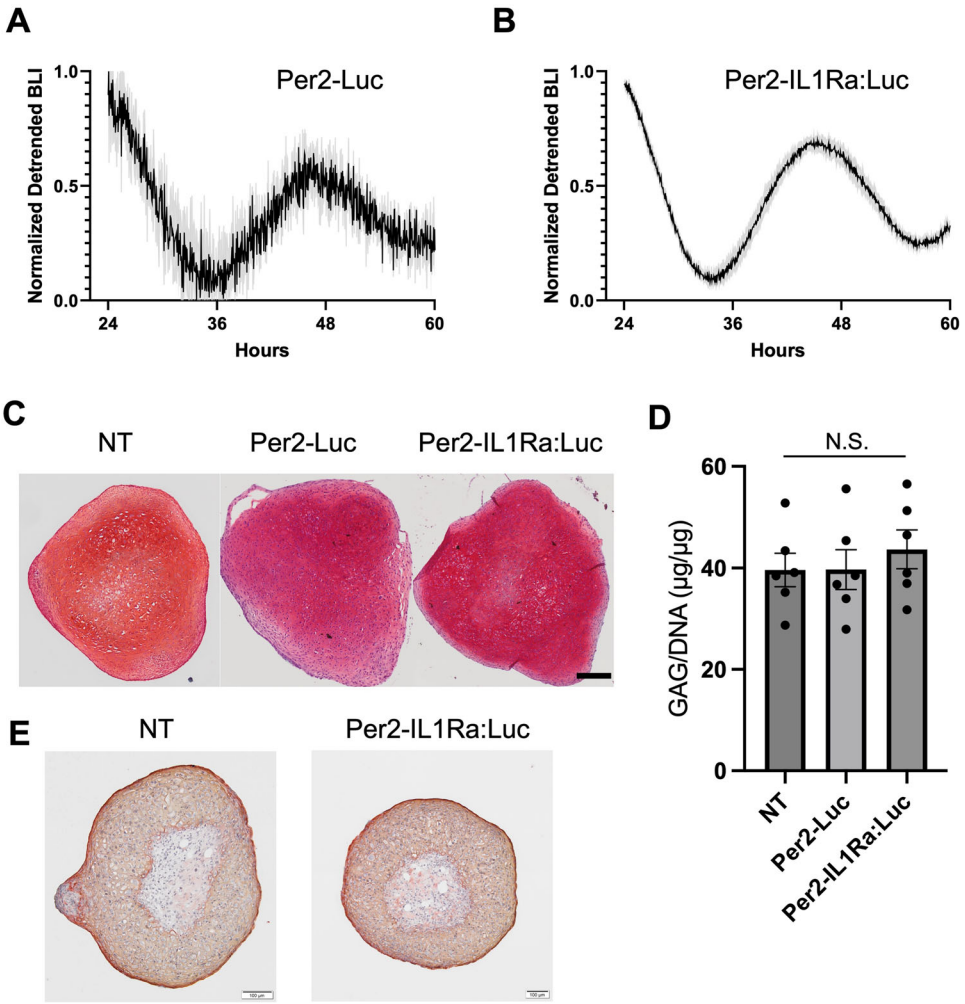

Fig. 2 | Characterization of chronogenetic reporter circuit and tissue engineered cartilage. A *Per2*-Luc bioluminescence intensity (BLI) in tissue engineered cartilage ($n = 3$). **B** *Per2*-IL1Ra:Luc BLI in tissue engineered cartilage ($n = 13$). **C** Safranin-O staining for sGAGs, an indicator of cartilage matrix integrity ($n = 4$/group, scale bar = 100 µM). **D** Quantification of sGAGs normalized to DNA content within each pellet ($n = 7$/group, mean ± SEM, one-way ANOVA). No significance between non-transduced (NT), *Per2*-Luc, and *Per2*-IL1Ra:Luc constructs (n.s.=no significance, ANOVA). **E** Immunohistochemistry for collagen II, a key component of articular cartilage ($n = 2$-3/group, scale bar=100 µM). Source data are provided as a Source Data file.

Tissue-engineered cartilage was used as the model delivery system because it is avascular, aneural, can easily be implanted, and can survive in any implant location[24,26,31]. Additionally, previous work showed that circadian rhythms are fully developed within tissue-engineered cartilage[24]. Tissue-engineered cartilage is also highly relevant to RA therapeutics because it can be used to produce locally acting IL-1Ra to the synovium. Implants engineered from control or genetically-engineered iPSCs showed chondrogenic differentiation, as evidenced by rich sGAG and collagen type II staining and expression of circadian rhythms. In previous studies, we have shown that naïve iPSCs do not exhibit circadian rhythms but develop daily rhythms as they undergo chondrogenesis[24]. Importantly, we saw that our anti-inflammatory chronogenetic circuit could maintain its circadian rhythm in the presence of inflammatory cytokine, IL-1. Previously, it has been reported that inflammatory cytokines disrupt the circadian clock[24,25,33] but that the administration of anti-inflammatory agents could restore the circadian clock. Therefore, our chronogenetic circuit is capable of being clock-preserving, which is important for its ability to deliver anti-inflammatory biologics at prescribed times of day. The maintenance of oscillations even in the presence of inflammation demonstrates the robustness of this system in response to inflammatory challenge, providing additional support for the applicability of this approach as a cell-based therapeutic to target inflammatory flares. Additionally, this type of clock-preserving system can be used as a tool to better understand the relationship between circadian rhythms and inflammation.

Engineered tissue constructs showed changes in the expression of *Il1rn* as well as rate of protein synthesis of IL-1Ra with a calculated period of ~23 h, whereas control specimens did not show expression or synthesis of IL-1Ra. These findings confirm the cell-autonomous nature of this chronogenetic gene circuit to drive circadian rhythms in chondrocytes which can be maintained over at least 72 h without exogenous stimuli for resynchronization[24,34].

Once implanted, we observed via bioluminescence that the constructs entrained with the intrinsic circadian rhythm of mice and synthesized roughly 4-fold higher concentrations of IL-1Ra in the serum during the light period (ZT 9) as compared to the dark period (ZT 17). Importantly, once the light/dark cycle for these mice was switched, the implants rapidly entrained to the new conditions and reversed the time of peak IL-1Ra synthesis. We directly measured IL1-Ra in vivo at peak and trough times estimated from the experiments described above, in which we indirectly assayed IL1-Ra via luciferase expression in vitro, in vivo, and IL-1Ra expression every two hours in vitro. All of these factors give us confidence that our peak and trough samples are

https://doi.org/10.1038/s41467-025-56584-5

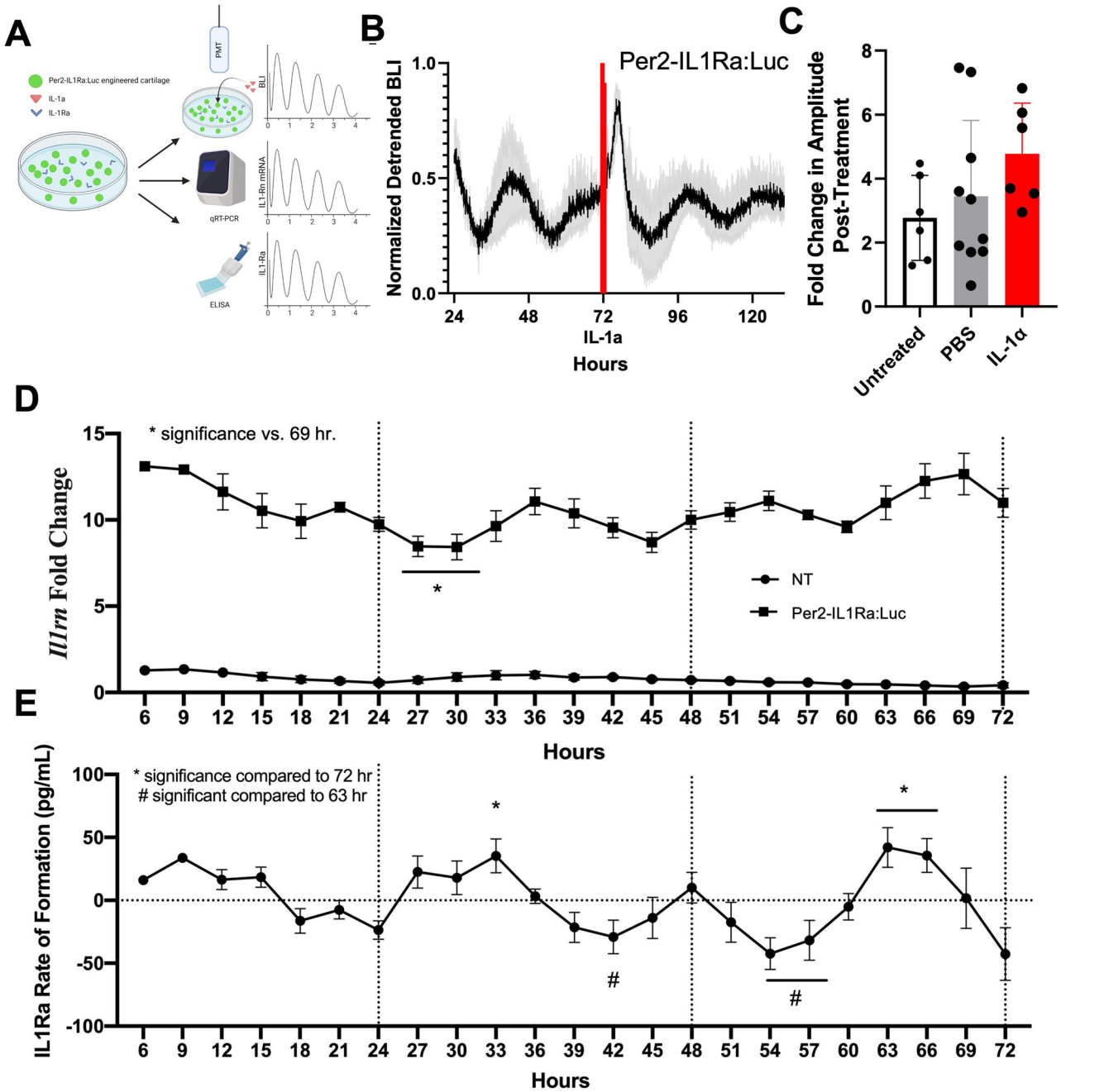

Fig. 3 | In vitro characterization of *Per2*-IL1Ra:Luc chronogenetic circuit. **A** Schematic of experiments. **B** BLI of *Per2*-IL1Ra:Luc constructs before and after addition of 1 ng/mL of IL-1α ($n = 6$). **C** Fold change in BLI amplitude of circadian oscillation from one day before to one day after IL-1 treatment compared to the same measurement in untreated cells ($n = 6$) and cells treated with PBS ($n = 18$) (no significance). **D** Gene expression analysis of *Il1rn* ($n = 6$/group, fold change relative to NT control at 0 h). Samples collected every 3 hours for 72 h. In the *Per2*-IL1Ra:Luc group there were oscillations of *Il1rn mRNA abundance* and a significant decrease in expression at 27 h ($p = 0.04$) and 39 h ($p = 0.03$) compared to peak expression at 69 hvia one-way ANOVA. Asterisks denotes significance compared to 69h. **E** IL-1Ra protein production over the course of 3 days in the *Per2*-IL1Ra:Luc circuits ($n = 6$). The chronogenetic circuit produced oscillating IL-1Ra levels (ARSER test, $p = 0.03$) with a significant decrease in expression at 42 h ($p = 0.04$), 57 h ($p = 0.004$), and 60 h ($p = 0.03$) compared to peak expression time of 63 h and a significant increase in expression at peak times 33 h ($p = 0.01$), 63 h ($p = 0.004$), and 66 h ($p = 0.01$) compared to 72 h via one-way ANOVA. Asterisks denotes significance compared to 72 h and hash denotes significance compared to 63 h. Source data are provided as a Source Data file. *Created in BioRender. Guilak, F. (2025)* https://BioRender.com/n75d206.

reliable measures of actual peak and trough IL-1Ra levels in vivo in implanted mice. These findings indicate the predictability and controllability of this system since the implants can rapidly entrain with the host's circadian clock. The chronogenetic circuits developed here were driven by core clock gene *Per2*, however other core clock genes can be used for alternative timed delivery or for specific inputs, such as *Bmal1* for antiphase and *Dbp/Nr1d1* for high amplitude. In situations where an increased concentration of protein is required, alternative promoters such as *Dbp/Nr1d1* can be used for higher amplitude and increased protein production. Additionally, targeted mutations in the *Per2* promoter can result in increased protein production. Alternatively, an increased concentration of lentivirus can be used to transduce the cells for increased protein production as well. Additionally, multiple circuits can be used with antiphase drivers to create a

https://doi.org/10.1038/s41467-025-56584-5

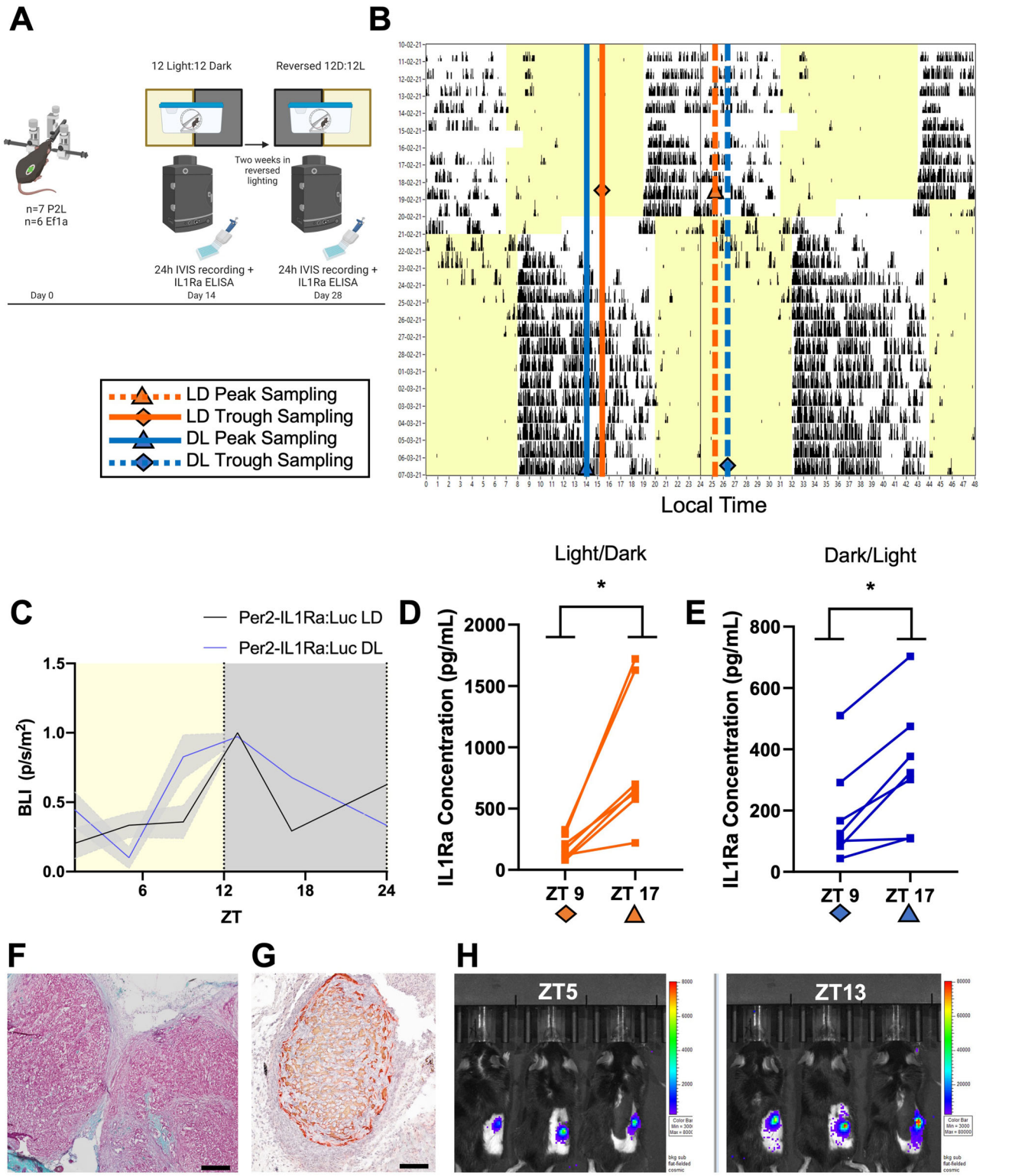

two-pronged approach with one drug delivered at multiple peaks throughout the day or for two different drugs to be delivered at different times, depending on the need in disease progression. Additionally, mutations can be made in core clock genes promoters in the E-box and/or D-box to delay or advance the phase of the circadian clock, to tailor this approach to any timing of delivery[35–37].

The creation of these chronogenetic therapies opens a new field of cell-based therapies and ways to enhance drug efficacy and mitigate side effects through the timed delivery of drugs personalized to the patient's circadian rhythm. By developing an in vitro system to characterize these chronogenetic gene circuits, we can characterize drug delivery intrinsic to the engineered cells and then test them in vivo for chronotherapy outcomes. Although circadian rhythms, clock-controlled genes, and their therapeutic potentials are starting to be better understood, there are still many unknowns on the effect the core circadian clock has on specific genes, and the importance of timed drug delivery. Therefore, these synthetic circuits can help unravel the links between circadian rhythms and disease progression.

Fig. 4 | In vivo characterization of *Per2*-IL1Ra-t2a-Luc chronotherapy circuit. **A** Schematic of experiments. **B** Mouse wheel-running actigraphy (black tick marks) recorded to monitor circadian entrainment to the light cycle. Yellow background is lights on; white background is lights off. IL-1Ra was measured from blood drawn in the day (ZT9, diamonds) and night (ZT 17, triangles) two days before and 15 days after a 12-h shift in the light cycle. Orange lines represent light/dark cycle sampling and blue lines represent dark/light sampling. **C** Bioluminescence from *Per2*-IL1Ra:Luc constructs implanted in mice peaked around dusk before and after adjusting to the reversed light cycle ($n = 7$ mice, 4 constructs/mouse). LD = light/dark cycle. DL = dark/light cycle. **D** Serum IL-1Ra concentration evaluated 4 h post BLI peak and trough expression (repeated measures t-test, $p = 0.0096$, $n = 6$ mice, 4 constructs/mouse). Asterisks denotes significance within each sample, between timepoints. **E** Serum IL-1Ra concentration evaluated 4 hours post BLI peak and trough expression (repeated measures t-test, $p = 0.004$, $n = 7$, 4 constructs/mouse). Asterisks denotes significance within each sample, between timepoints. **F** Safranin-O staining of a representative engineered cartilage construct 21 days after implantation. Image is from one implant after removal and staining. Scale bar = 100 µm, 6 replicates. **G** Immunohistochemistry staining for collage type II of a representative engineered cartilage construct 21 days after implantation. Image is from an implant after removal and staining. Scale bar = 200 µm, 6 replicates. **H** Bioluminescence images of three mice bearing *Per2*-IL1Ra:Luc flank implants, taken around the peak (ZT13) and trough (ZT5) of *Per2* expression. Source data are provided as a Source Data file. Created in BioRender. *Created in BioRender. Guilak, F. (2025)* https://BioRender.com/m89a345.

Additionally, these systems can be used to deliver anabolic factors to cells to create better tissue engineered systems, as well as can be used to create in vitro model systems that can accurately depict cyclic disease states to better understand the effects of time. To ensure the ability to turn off these chronogenetic therapies when implanted, in the case of adverse effects, we could incorporate a system such as a Tet-on or Tet-off switch into the cells[38]. In this case, the oral administration of a tetracycline analog such as doxycycline could be used to selectively activate or inactivate drug delivery from the therapeutic gene circuit.

This study provides proof-of-concept of a chronogenetic gene circuit for programmed circadian drug delivery. In the future, we may be able to combine this type of circadian therapy with biomaterials-based delivery systems [e.g.[39,40],] for controlled delivery of complex combinations of drugs at specific times of day to enhance efficacy. Future work will be directed toward testing this system in disease models with inflammatory flares, such as RA, and evaluate the efficacy of this approach compared to antibody treatments, the current treatment for RA. Such approaches can also be expanded to create chronogenetic therapies for many different tissues and targeting different diseases where there are therapeutic targets for clock-controlled genes. Together, this framework for developing personalized chronogenetic therapies is an approach to establish a new generation of cell therapies that provide precise and effective therapeutic drug delivery.

Methods

Reagent sources

A list of reagents and their sources and catalog numbers are provided in Supplementary Dataset 1.

Murine induced pluripotent stem cell culture and differentiation

All animal procedures were performed with approval of the Washington University Institutional Animal Care and Use Committee (IACUC, protocol 19-0758). Murine induced pluripotent stem cells (miPSCs) were derived from tail fibroblasts from male adult C57BL/6 mice and transduced with a single lentiviral vector controlling the transgenic expression of mouse *Oct4* (*Pou5f1*), *Sox2*, *Klf4*, and *c-Myc*. Tail fibroblasts from C57BL/6 mice were isolated by removing the outer layer of skin, mincing the tissue, and digesting it overnight in 0.2% collagenase type I (Worthington Biochemical). The digested cells were then passaged several times in DMEM-LG (Sigma-Aldrich) supplemented with 15% fetal bovine serum (FBS, Sigma-Aldrich) and 1% penicillin-streptomycin-fungizone (P/S/F, Gibco). To prepare the feeder layer, mouse embryonic fibroblasts (PMEF-NL, Millipore) were treated with 10 µg/ml mitomycin-C (Sigma-Aldrich) for 2–3 h to inhibit proliferation, then cultured on 0.1% gelatin-coated dishes at confluence. Reprogramming was initiated by transducing tail fibroblasts with a doxycycline-inducible lentiviral vector carrying mouse cDNAs for Oct4 (Pou5f1), Sox2, Klf4, and c-Myc for 24 h. After approximately two weeks, individual colonies were manually selected based on their morphology and maintained on feeder cells in iPSC media without doxycycline.

Undifferentiated iPSCs were analyzed for pluripotency by their ability to form teratomas by injection of cells into the kidney and testis of three separate mice as described reported[41,42]. miPSCs were cultured in Dulbecco's Modified Eagle's Medium High Glucose (DMEM-HG, Gibco, 11965092), 20% lot selected fetal bovine serum (FBS, R&D Systems, S11510), 100 nM minimum essential medium nonessential amino acids (NEAA, Gibco, 11140035), 55 µM 2-mercaptoethanol (2-me, Gibco, 21985023), 24 ng/mL gentamicin (Gibco, 15710064), and 1000 U/mL mouse leukemia inhibitory factor (LIF, Sigma-Aldrich, ESG1107), and maintained on mitomycin C (Sigma-Aldrich, M4287)-treated mouse embryonic fibroblasts (Millipore, PMEF-NL).

Feeder layer cells were removed through two subtraction steps of 45 min each on tissue culture plastic, separated by a day of culture on 0.1% gelatin (Sigma-Aldrich). Cells were resuspended at 2×10^7 cells/ml, and micromasses were established by plating 2×10^5 iPSCs in 10 µl into individual wells of 48-well plates (Corning) or as a set of 30 micromasses in a 10 cm dish (BD). After a 2–3 h incubation, additional iPSC medium with 10% serum (without LIF) was added. Twenty-four hours later, the media was switched to serum-free chondrogenic differentiation medium. miPSCs were differentiated toward a mesenchymal state using a high-density micromass culture[42] in medium consisting of DMEM-HG, 1% culture medium supplement containing recombinant human insulin, human transferrin, and sodium selenite (ITS + , Corning, 354352), 100 nM NEAA, 55 µM 2-me, 24 ng/mL gentamicin, 50 µg/mL L-ascorbic acid (Sigma-Aldrich, A8960), and 40 µg/mL L-proline (Sigma-Aldrich, P5607). On days 3–5, this medium was supplemented with 100 nM dexamethasone (Sigma-Aldrich, D4902) and 50 ng/mL bone morphogenetic protein 4 (BMP-4; R&D Systems, 5020-BP-010). After 15 days, the micromasses were dissociated with pronase (Millipore Sigma, 53702) and collagenase type II (Worthington Biochemical, LS004177). Cells were centrifuged, incubated with 0.25% trypsin-EDTA (Sigma-Aldrich) for 5 min, and resuspended in sort medium containing DMEM-HG, 2% FBS, DNase I, 10 mM HEPES (Gibco), 2× P/S/F, and 33.3 nM propidium iodide (Biolegend) as a dead cell marker. The pre-differentiated iPSCs (PDiPSCs) were plated on gelatin-coated dishes in expansion medium containing DMEM-HG, 10% lot selected FBS, 1% ITS + , 100 nM NEAA, 55 µM 2-me, 1% penicillin/streptomycin (P/S, Gibco, 15140122), 50 µg/mL L-ascorbic acid, 40 µg/mL L-proline, and 4 ng/mL of basic fibroblast growth factor (bFGF, R&D Systems, 3718-FB).

Cells were plated at 1×10^4 cells/cm^2 on gelatin-coated plates in chondrogenic expansion medium, which consists of chondrogenic differentiation medium with 10% FBS and 4 ng/ml bFGF (Roche). Cells were passaged upon reaching sub-confluence every 2–3 days using 0.05% trypsin-EDTA (Sigma-Aldrich). After each passage, cells were used to form pellets by centrifuging 2.5×10^5 cells at 200 × g for 5 min in 15 ml tubes. To create cartilage implants, passage 2 PDiPSCs were pelleted by centrifugation of 250 K cells[42]. Constructs were cultured

for 14–21 days in chondrogenic medium consisting of DMEM-HG, 1% ITS + , 100 nM NEAA, 55 µM 2-me, 1% P/S, 50 µg/mL L-ascorbic acid, 40 µg/mL L-proline, 100 nM dexamethasone, and 10 ng/mL TGF-β3 (R&D Systems, 8420-B3).

Cell-based chronogenetic circuit design

We developed a lentiviral system activated by *Per2* expression, a core circadian clock gene. The vector contained a t2a component that linked luciferase (Luc) downstream of the transgene, with the goal of creating a chronotherapy circuit that had its own luciferase reporter system. Therefore, upon activation of the circadian clock and subsequent activation of *Per2*, the chronogenetic circuit would be activated and produce interleukin-1 receptor antagonist (*Per2*-IL1Ra:Luc) over a 24-h period.

The murine *Per2* promoter was obtained from lentiviral *Per2*-Luc plasmid[33]. This *Per2* promoter contains the essential clock-regulated E-box sequence sufficient to drive rhythmic gene transcription and translation. This promoter was cloned in place of the CMV promoter in a CMV-GFP-t2a-Luc lentiviral cassette (Systems Biosciences, BLIV101PA-1). The CMV promoter was removed with restriction enzymes and the *Per2* promoter was incorporated using Gibson Assembly[43]. Murine interleukin-1 receptor antagonist (IL-1Ra) was incorporated into the *Per2*-GFP-t2a-Luc cassette in place of GFP through restriction enzyme removal of GFP and Gibson Assembly[43] to incorporate IL-1Ra. The IL-1Ra was obtained from a plasmid created to sense and respond to inflammation[24,31,44]. This lentiviral circuit was then able to produce IL-1Ra and luciferase in response to *Per2* activation (*Per2*-IL1Ra:Luc) and can be used as an anti-inflammatory therapeutic.

Lentivirus production and cell transduction

Human embryonic kidney (HEK) 293 T cells (ATCC, CRL-11268) were co-transfected with second-generation packaging plasmid psPAX2 (Addgene, 12260), the envelope plasmid pMD2.G (Addgene, 12259), and the expression transfer vector (*Per2*-IL1Ra:Luc) by calcium phosphate precipitation to make vesicular stomatitis virus glycoprotein pseudotyped lentivirus[45]. The lentivirus was harvested at 24- and 48-hours post transfection and stored at -80 °C until use. The functional titer of the virus was determined with quantitative real-time polymerase chain to determine the number of lentiviral DNA copies integrated into the genome of transduced HeLa cells (ATCC, CCL-2)[45]. PDiPSCs were transduced before being pelleted. For PDiPSC transductions, virus was thawed on ice and diluted in medium to obtain the desired number of viral particles to achieve a multiplicity of infection of 3[44]. Polybrene (Sigma-Aldrich, TR-1003) was added to a concentration of 4 µg/mL to aid in transduction. The medium of the cells was aspirated and replaced with virus-containing medium, and cells were incubated for 24 h before aspirating the viral medium.

In vitro characterization of chronotherapy circuits

All chronotherapy circuits were characterized in vitro after development of tissue-engineered cartilage constructs following 14 days in chondrogenic culture. The chronogenetic tissue-engineered constructs, *Per2*-Luc control, and EF1α-Luc (a constitutive luciferase control) constructs were subject to bioluminescence recordings to track circadian oscillations. Media from the *Per2*-IL1Ra:Luc constructs was collected every 3 h for 72 h to determine IL-1Ra production, and *Per2*-IL1Ra:Luc and non-transduced (NT) control constructs were harvested every 3 h for 72 h for *Il1rn* gene expression.

Bioluminescence recordings and imaging

Tissue-engineered cartilage constructs (*Per2*:Luc, EF1α-Luc, or *Per2*-IL1Ra:Luc) were plated in 35 mm petri dishes (Thermo Scientific, 150318) with 1 mL of recording medium containing D-luciferin (Goldbio, eLUCK-1G), sealed with vacuum grease, and placed in a light-tight 36 °C incubator containing photo-multiplier tubes (PMTs) (Hamamatsu Photonics, H8259-01). Each dish was placed under one PMT and the bioluminescence was recorded as photons per 180 s. Bioluminescence data were detrended with a 24 h moving average and analyzed in ChronoStar 1.0[46]. Recording medium contained DMEM powder (Sigma-Aldrich, D5030), B27 supplement (Gibco, 17504044), P/S, L-glutamine (Thermo Scientific, J60573.14), HEPES (Sigma-Aldrich, H0887-100ML), and D-glucose (Thermo Scientific, A16828.0 C).

Additionally, *Per2*-IL1Ra:Luc constructs were imaged in recording medium for 72 h using an Andor iKon-M electron multiplying charged coupled device (Oxford Instruments, iKON-M 934 CCD) at 20× magnification with 1 h exposure time and 2 × 2 binning. During multi-day recordings, samples were maintained at 36 °C in darkness. Image sequences were concatenated into videos using ImageJ and individual cells were visualized for bioluminescence output.

Gene expression with quantitative real time polymerase chain reaction

Per2-IL1Ra:Luc and non-transduced (NT) control constructs were collected every 3 h for 72 h. Cartilage constructs were homogenized using a miniature beat beater (Biospec Products, 112011), lysed in Buffer RL, and RNA was isolated following the manufacturer's protocol (Total RNA Purification Plus Kit; Norgen Biotek, 48300). Reverse transcription was performed using Superscript VILO complementary DNA master mix (Invitrogen, 11755050). qRT-PCR was performed using Fast SyBR Green master mix (Applied Biosystems, 4385616). Primer pairs were synthesized by Integrated DNA Technologies, Inc: *Il1rn* [forward (F), 5′-GTCCAGGATGGTTCCTCTGC-3′; reverse (R), 5′-TCTTCCGGT GTGTTGGTGAG-3′] and *r18s* [F, 5′-CGGCTACCACATCCAAGGAA-3′; R, 5′-GGGCCTCGAAAGAGTCCTGT-3′]. Data are reported as fold changes with a 6 h moving average and were calculated using the $\Delta\Delta C_T$ method and are shown relative to the non-transduced (NT) control group at 0 hours and ribosomal 18 s was used as the reference gene.

Enzyme-linked immunosorbent assays

Media from *Per2*-IL1Ra:Luc constructs was collected every 3 h for 72 h and stored at −20 °C. IL-1Ra concentration was measured with DuoSet enzyme-linked immunosorbent assay (ELISA) specific to mouse IL-1Ra/IL-1F3 (R&D Systems, DY480). Data are reported as rates of formation with a 6 h moving average to account for accumulation of IL-1Ra in the media over time.

Histological, biochemical analysis, and immunohistochemistry of tissue-engineered cartilage

After 14 days of chondrogenic culture constructs were washed with PBS (Gibco, 14040133) and fixed in 10% NBF (Sigma-Aldrich, HT501128) for 24 h, paraffin embedded, and sectioned at 8 µm thickness. Slides were stained for Safranin-O (Sigma-Aldrich, HT904), hematoxylin (Fisher Scientific, NC9064721), fast green (Electron Microscopy Biosciences, 15500)[47]. In vivo implants were removed from mice after 21 days and fixed in 4% PFA (Electron Microscopy Biosciences, 15710) for 24 h, paraffin embedded, and sectioned at 8 µm thickness. Slides were stained for Safranin-O/hematoxylin/fast green[47].

For biochemical analysis, cartilage constructs were digested overnight in 125 µg/mL papain at 65°C. DNA content was measured with PicoGreen assay (Invitrogen, P11495) and total sulfated glycosaminoglycan (sGAG) content was measured using a 1,9-dimethylmethylene blue (Sigma-Aldrich, 341088) assay at 525 nm wavelength[48].

For immunohistochemistry to detect collagen II paraffin sections of the cartilage constructs, either taken down after 14 days of chondrogenic culture or removed from mice after 21 days, were incubated for 3 minutes at 37 °C with proteinase K (10 µg/mL; New England BioLabs, P8107S) diluted in 10 mM tris-HCL/EDTA (TE Buffer, pH 8.0; Sigma-Aldrich, 93283) for antigen retrieval. The slides were then treated with 3% peroxidase H_2O_2 in methanol for 30 minutes and

blocked with 10% goat serum (ThermoFisher, 50197Z) for 30 min at room temperature. Primary antibody Col2 (University of Iowa, II-II6B3) were diluted in 1% bovine serum albumin (BSA) to a concentration of 1:1 and incubated for 1 h at room temperature. The secondary antibody, peroxidase-conjugated goat anti-mouse immunoglobulin G (Abcam, 97021) was diluted in 1:500 in 1% BSA and incubated at room temperature for 30 minutes. Negative controls did not receive the primary antibody. All slides were counterstained with Vector Hematoxylin QS (Vector Lab, H3404).

Inflammatory challenge

Per2-IL1Ra:Luc constructs were subjected to an inflammatory challenge using 1 ng/mL IL-1α (R&D Systems, 200-LA). These constructs were cultured in recording medium, and their bioluminescence was monitored for a duration of 72 hours, as described previously[24,25]. Following this initial recording period, IL-1α was introduced to the culture dish, and bioluminescence was further monitored for an additional 72 h. Samples meeting the criteria of exhibiting bioluminescence within the 18–32-h timeframe, with a mean bioluminescence exceeding 30,000 photons, and a pre-cytokine amplitude surpassing 20,000 photons were included in the subsequent analysis. Damping, characterized by the natural decline in amplitude over time in the absence of external entraining cues, was considered. The alteration in amplitude resulting from IL-1α treatment was quantified by assessing the fold change in amplitude between the 24 h preceding and the 48 h following the treatment (pre-treatment amplitude divided by post-treatment amplitude).

In vivo characterization of chronotherapy circuits

Per2-IL1Ra:Luc or EF1α-Luc constructs were implanted into mice subcutaneously for circuit characterization and evaluation of therapeutic effect. C57BL/6 J mice ($n = 7$, 10 weeks old; Jackson Laboratory, 000664) were anesthetized using 2% isoflurane. The fur was trimmed in a 1 cm × 1 cm area of fur, the skin was sterilized using a betadine wash, and a small incision 0.5 cm long was made, not extending into muscle or fat tissue. A sterile spatula was inserted into the incision to create a 0.5 × 0.5 cm pocket below the skin and 4 cell pellets were transferred into the pocket. We used 8-0 vicryl sutures (Johnson & Johnson J401G) to close the incision, applied antibiotic ointment, injected analgesic carprofen (5 mg/kg, subcutaneously), and allowed the mouse to regain consciousness in the home cage placed on a heating pad. Mice were monitored and given additional analgesic for three days post implant. No mice died during implant or prior to experiment completion. Mice were maintained on a standard dark/light cycle with 7am lights on/7 pm lights off at room temperature (22 °C) at ambient humidity (not measured). All procedures were approved by the Institutional Anmical Care and Use Committe (IACUC) at Washington University in St. Louis (Protocol #19-0758).

Per2-IL1Ra:Luc entrainment characterization

Per2-IL1Ra-t2a-Luc implants were characterized based on ability to entrain to mouse circadian rhythms through mouse actigraphy collection and bioluminescence imaging. Additionally, the ability for the *Per2*-IL1Ra:Luc circuit to produced IL-1Ra in a timed manner was evaluated through IL-1Ra serum concentration.

Mice were subjected to normal light/dark cycle and wheel running activity was tracked. Bioluminescence was imaged every 4 h for 36 h (IVIS Lumina III, Perkin Elmer, CLS136334). After bioluminescence imaging, the peak and trough luminescence of implants were determined to be ZT 13 and ZT 5, respectively. To account for IL-1Ra translation, blood draws were taken from mice 4 h after luminescence peak and trough through submandibular blood serum collection. IL-1Ra serum levels were assessed by ELISA (Quantikine-IL1Ra; R&D Systems, DRA00B).

To evaluate if constructs have the ability to continue to entrain to mice circadian rhythm, mice were phase delayed 12 h using a reversed light/dark schedule. Actigraphy data was collected continuously to monitor entrainment of activity and after 14 days, constructs were again imaged for bioluminescence every 4 h for 36 h. Consistent with two weeks prior, the peak and trough luminescence were determined to be at ZT 5 and ZT 13. Additionally, serum was collected at the peak and trough of bioluminescence expression and IL-1Ra serum was quantified by ELISA.

Additionally, EF1α-Luc constructs were implanted into 6 mice (4 implants/mouse) and bioluminescence was tracked under a light/dark cycle in the same manner as the mice implanted with *Per2*-IL1Ra:Luc constructs. These were used as a control to ensure the oscillatory nature of the chronogenetic circuits was driven by *Per2*.

To provide further evidence that *Per2*-IL1Ra:Luc maintains circadian oscillation over time and that EF1α-Luc does not show circadian oscillation, we conducted long term in vivo bioluminescence recordings. Pellets were implanted as described above. Immediately after pellet implantation, mice were individually placed in constant darkness in a light tight box containing two photomultiplier tubes (PMT, Hamamatsu H8259-01, Lumicycle In Vivo, Actimetrics)[49]. Mice received luciferin in their water (10 mM, Gold Biotechnology) ad libitum over the 3 days of recording. This method allowed for recording of *Per2* or Ef1-alpha luciferase expression in freely moving mice. A sum of the signal obtained every minute from the two PMTs was used to determine overall counts following a dark count correction. Dark counts were collected for 1 min every 15 min by closing the programmable shutter during that 1 min. Animals were checked daily to ensure that they had adequate food and water.

Statistical analysis

Statistical analysis was performed using Prism (Version 9.4.1, GraphPad Software). A one-way ANOVA with Tukey's HSD post hoc test was used to analyze IL-1Ra concentration and *Il1rn* expression ($\alpha = 0.05$) in IL1Ra:Luc circuits in vitro. Additionally, MetaCycle, specifically the ARSER test, was used to analyze IL-1Ra concentration and *Il1rn* expression ($\alpha = 0.05$)[50]. For biochemistry data, a one-way ANOVA with Dunnett's post hoc test was used with NT as the control ($\alpha = 0.05$). In vivo IL-1Ra serum was analyzed with a paired t-test ($\alpha = 0.05$). A one-way ANOVA with Fisher's LSD post hoc test was used to analyze change in amplitude for constructs treated with IL-1α with untreated constructs and PBS-treated constructs ($\alpha = 0.05$).

For in vitro bioluminescence recordings, Chronostar (Version 1.0) was used to detrend the data with a 24 h moving average and calculated Circadian R^2 value, a correlation coefficient with a cosine curve. Values of 0.8 or higher are considered circadian. Bioluminescence traces from freely moving mice were analyzed using Chronostar 1.0, as described for in vitro bioluminescence traces.

Reporting summary

Further information on research design is available in the Nature Portfolio Reporting Summary linked to this article.

Data availability

All data are contained within the manuscript and supplementary information. Source data are provided with this paper.

Code availability

No custom code was used in the analysis of this study; all code is available as referenced in the Methods.

References

1. Selfridge, J. M. et al. Chronotherapy: intuitive, sound, founded...but not broadly applied. *Drugs* **76**, 1507–1521 (2016).

2. Hastings, M. H., Reddy, A. B. & Maywood, E. S. A clockwork web: circadian timing in brain and periphery, in health and disease. *Nat. Rev. Neurosci.* **4**, 649–661 (2003).
3. Takahashi, J. S., Hong, H. K., Ko, C. H. & McDearmon, E. L. The genetics of mammalian circadian order and disorder: implications for physiology and disease. *Nat. Rev. Genet.* **9**, 764–775 (2008).
4. Roenneberg, T. & Merrow, M. Circadian clocks - the fall and rise of physiology. *Nat. Rev. Mol. Cell Biol.* **6**, 965–971 (2005).
5. Dudek, M. & Meng, Q. J. Running on time: the role of circadian clocks in the musculoskeletal system. *Biochem* **463**, 1–8 (2014).
6. Yoo, S. H. et al. PERIOD2::LUCIFERASE real-time reporting of circadian dynamics reveals persistent circadian oscillations in mouse peripheral tissues. *Proc. Natl. Acad. Sci. USA* **101**, 5339–5346 (2004).
7. Patke, A., Young, M. W. & Axelrod, S. Molecular mechanisms and physiological importance of circadian rhythms. *Nat. Rev. Mol. Cell Biol.* **21**, 67–84 (2020).
8. Cutolo, M. S., Craviotto, B., Pizzorni, C. & Sulli, C. A. Circadian rhythms in RA. *Ann. Rheum. Dis.* **62**, 593–596 (2003).
9. Keller, M. et al. A circadian clock in macrophages controls inflammatory immune responses. *Proc. Natl. Acad. Sci. USA* **106**, 21407–21412 (2009).
10. Ruben, M. D. et al. A database of tissue-specific rhythmically expressed human genes has potential applications in circadian medicine. *Sci. Transl. Med.* **10** https://doi.org/10.1126/scitranslmed.aat8806 (2018).
11. Zhang, R., Lahens, N. F., Ballance, H. I., Hughes, M. E. & Hogenesch, J. B. A circadian gene expression atlas in mammals: implications for biology and medicine. *Proc. Natl. Acad. Sci. USA* **111**, 16219–16224 (2014).
12. Andersson, M. L. et al. Diurnal variation in serum levels of cartilage oligomeric matrix protein in patients with knee osteoarthritis or rheumatoid arthritis. *Ann. Rheum. Dis.* **65**, 1490–1494 (2006).
13. Cutolo, M. Circadian rhythms and rheumatoid arthritis. *Jt. Bone Spine* **86**, 327–333 (2019).
14. Kong, S. Y. S. et al. Diurnal variation of serum and urine biomarkers in patients with radiographic knee osteoarthritis. *Arthritis Rheum.* **54**, 2496–2504 (2006).
15. Buttgereit, F., Smolen, J. S., Coogan, A. N. & Cajochen, C. Clocking in: chronobiology in rheumatoid arthritis. *Nat. Rev. Rheumatol.* **11**, 349–356 (2015).
16. Levi, F., Le Louarn, C. & Reinberg, A. Timing optimizes sustained-release indomethacin treatment of osteoarthritis. *Clin. Pharm. Ther.* **37**, 77–84 (1985).
17. Lemmer, B. The clinical relevance of chronopharmacology in therapeutics. *Pharm. Res* **33**, 107–115 (1996).
18. Sobrino, J., Casanas, L., Izquierdo, C. & Clavell, J. Circadian rhythm variability in arterial blood pressure. *Rev. Enferm.* **29**, 50–52 (2006).
19. Smolensky, M. H., Lemmer, B. & Reinberg, A. E. Chronobiology and chronotherapy of allergic rhinitis and bronchial asthma. *Adv. Drug Deliv. Rev.* **59**, 852–882 (2007).
20. Damato, A. R. et al. Temozolomide chronotherapy in patients with glioblastoma: a retrospective single institute study. *Neuro-Oncol. Adv.* https://doi.org/10.1093/noajnl/vdab041 (2021).
21. Zvonic, S. et al. Circadian oscillation of gene expression in murine calvarial bone. *J. Bone Min. Res.* **22**, 357–365 (2007).
22. Kaur, G., Phillips, C., Wong, K. & Saini, B. Timing is important in medication administration: a timely review of chronotherapy research. *Int. J. Clin. Pharm.* **35**, 344–358 (2013).
23. Stefanov, B. A. & Fussenegger, M. Biomarker-driven feedback control of synthetic biology systems for next-generation personalized medicine. *Front Bioeng. Biotechnol.* **10**, 986210 (2022).
24. Pferdehirt, L. et al. Synthetic gene circuits for preventing disruption of the circadian clock due to interleukin-1-induced inflammation. *Sci. Adv.* **8**, eabj8892 (2022).
25. Guo, B. et al. Catabolic cytokines disrupt the circadian clock and the expression of clock-controlled genes in cartilage via an NFsmall ka, CyrillicB-dependent pathway. *Osteoarthr. Cartil.* **23**, 1981–1988 (2015).
26. Choi, Y. R. et al. A genome-engineered bioartificial implant for autoregulated anticytokine drug delivery. *Sci. Adv.* **7**, eabj1414 (2021).
27. Douma, L. G. & Gumz, M. L. Circadian clock-mediated regulation of blood pressure. *Free Radic. Biol. Med.* **119**, 108–114 (2018).
28. Chen, H. C. et al. Disrupted expression of circadian clock genes in patients with bronchial asthma. *J. Asthma Allergy* **14**, 371–380 (2021).
29. Nosal, C., Ehlers, A. & Haspel, J. A. Why lungs keep time: circadian rhythms and lung immunity. *Annu Rev. Physiol.* **82**, 391–412 (2020).
30. Coleman, J. L. et al. Diurnal variations in articular cartilage thickness and strain in the human knee. *J. Biomech.* **46**, 541–547 (2013).
31. Nims, R. J. et al. A synthetic mechanogenetic gene circuit for autonomous drug delivery in engineered tissues. *Sci. Adv.* **7** https://doi.org/10.1126/sciadv.abd9858 (2021).
32. Pando, M. P., Morse, D., Cermakian, N. & Sassone-Corsi, P. Phenotypic rescue of a peripheral clock genetic defect via SCN hierarchical dominance. *Cell* **110**, 107–117 (2002).
33. Dudek, M. et al. The intervertebral disc contains intrinsic circadian clocks that are regulated by age and cytokines and linked to degeneration. *Ann. Rheum. Dis.* **76**, 576–584 (2017).
34. Dudek, M. et al. The chondrocyte clock gene Bmal1 controls cartilage homeostasis and integrity. *J. Clin. Invest.* **126**, 365–376 (2016).
35. Patke, A. et al. Mutation of the human circadian clock gene CRY1 in familial delayed sleep phase disorder. *Cell* **169**, 203–215.e213 (2017).
36. Jones, C. R., Huang, A. L., Ptacek, L. J. & Fu, Y. H. Genetic basis of human circadian rhythm disorders. *Exp. Neurol.* **243**, 28–33 (2013).
37. Ashbrook, L. H., Krystal, A. D., Fu, Y. H. & Ptacek, L. J. Genetics of the human circadian clock and sleep homeostat. *Neuropsychopharmacology* **45**, 45–54 (2020).
38. Das, A. T., Tenenbaum, L. & Berkhout, B. Tet-on systems for doxycycline-inducible gene expression. *Curr. Gene Ther.* **16**, 156–167 (2016).
39. Tibbitt, M. W. & Anseth, K. S. Dynamic microenvironments: the fourth dimension. *Sci. Transl. Med.* **4**, 160ps124 (2012).
40. Wechsler, M. E. et al. Engineered microscale hydrogels for drug delivery, cell therapy, and sequencing. *Biomed. Microdevices* **21**, 31 (2019).
41. Carey, B. W. et al. Reprogramming of murine and human somatic cells using a single polycistronic vector. *Proc. Natl. Acad. Sci. USA* **106**, 157–162 (2009).
42. Diekman, B. O. et al. Cartilage tissue engineering using differentiated and purified induced pluripotent stem cells. *Proc. Natl. Acad. Sci. USA* **109**, 19172–19177 (2012).
43. Gibson, D. G. et al. Enzymatic assembly of DNA molecules up to several hundred kilobases. *Nat. Methods* **6**, 343–345 (2009).
44. Pferdehirt, L., Ross, A. K., Brunger, J. M. & Guilak, F. A synthetic gene circuit for self-regulating delivery of biologic drugs in engineered tissues. *Tissue Eng. Part A* **25**, 809–820 (2019).
45. Salmon, P. & Trono, D. Production and titration of lentiviral vectors. *Curr. Protoc. Hum. Genet.* **Chapter 12**, Unit 12 10 https://doi.org/10.1002/0471142905.hg1210s54 (2007).
46. Maier, B., Loernzen, S., Finger, A., Herzel, H., & Kramer, A. Searching novel clock genes using RNAi-based screening. *In Circadian Clocks, Methods and Protocols, Brown, S.A.* **Chapter 8** (2020).
47. Estes, B. T., Diekman, B. O., Gimble, J. M. & Guilak, F. Isolation of adipose-derived stem cells and their induction to a chondrogenic phenotype. *Nat. Protoc.* **5**, 1294–1311 (2010).
48. Farndale, R. W., Buttle, D. J. & Barrett, A. J. Improved quantitation and discrimination of sulphated glycosaminoglycans by use of

dimethylmethylene blue. *Biochim. Biophys. Acta* **883**, 173–177 (1986).
49. Martin-Burgos, B. et al. Methods for detecting PER2:LUCIFERASE bioluminescence rhythms in freely moving mice. *J. Biol. Rhythms* **37**, 78–93 (2022).
50. Wu, G., Anafi, R. C., Hughes, M. E., Kornacker, K. & Hogenesch, J. B. MetaCycle: an integrated R package to evaluate periodicity in large scale data. *Bioinformatics* **32**, 3351–3353 (2016).

Acknowledgements

This work was supported by the Shriners Hospitals for Children (F.G.), the National Institutes of Health AR078949, AG15768, AG46927, AR080902, AR072999, AR073752, and AR074992 (to F.G.), and NIH GM131403 (to E.D.H.), the Philip and Sima Needleman Fellowship from the Washington University Center of Regenerative Medicine (to L.P.), a NIH NRSA fellowship (F31CA250161 to A.D.), a Versus Arthritis Senior Research Fellowship Award (20875 to Q.J.M.), and a Medical Research Council, UK (MRC) grant (MR/K019392/1 to Q.J.M.). Figures 3a and 4a, and S1a were generated in part using the BioRender software package.

Author contributions

L.P. and F.G. conceived the project. L.P., A.D., E.H., Q.J.M., and F.G. designed the experiments. L.P. designed the chronogenetic circuits and conducted *Il1rn* and IL1Ra tracking experiments. L.P. and A.D. conducted the circadian development and tissue engineered cartilage inflammatory challenge experiments. L.P., A.D., K.L., M.F.G.A., and D.P. conducted the in vivo experiments. L.P. and F.G. wrote the manuscript. All authors read, edited, and approved the final manuscript.

Competing interests

Farshid Guilak is an employee and shareholder in Cytex Therapeutics, Inc. Farshid Guilak and Lara Pferdehirt are co-inventors of US Patent Application No. 18/284,487 entitled "Compositions and Methods for Cell-Based Delivery Systems" (currently pending). relating to the development of chronogenetic gene circuits used in this study. Anna R. Damato, Kristin L. Lenz, Maria F. Gonzalez-Aponte, Daniel Palmer, Qing-Jun Meng, Erik D. Herzog declare no competing interests.

Additional information

Supplementary information The online version contains supplementary material available at https://doi.org/10.1038/s41467-025-56584-5.

Correspondence and requests for materials should be addressed to Farshid Guilak.

Peer review information *Nature Communications* thanks Ning Li, Alper Okyar, Stina Simonsson and the other anonymous, reviewer(s) for their contribution to the peer review of this work. A peer review file is available.